ISSN impresa 0717-3644
ISSN online 0718-221X

Maderas. Ciencia y tecnología 2023 (25): 23, 1-10

DOI: 10.4067/s0718-221x2023000100423

ANTIQUE WOOD PREPARATION BY INORGANIC SALTS TREATMENT AND ITS PERFORMANCE

Ming Sun[1]

https://orcid.org/0000-0001-5286-9355

Chencheng Zhao[1]

https://orcid.org/0000-0001-6607-8714

Courage Alorbu[2]

https://orcid.org/0000-0001-5193-4290

Lili Cai[2]

https://orcid.org/0000-0002-2099-4837

Youming Yu[1,♠]

https://orcid.org/0000-0002-2184-8890

ABSTRACT

Conservation of historic timber structures is of great importance for cultural inheritance and community identity promotion. However, most of the current methods available for ancient architecture protection significantly affect their original appearance and aesthetic value and finding wood elements that are similar to the ones in existing historic timber structures is not easy. Here we report a simple and effective method to archaize wood, *Castanopsis sclerophylla,* by ferric chloride ($FeCl_3$) treatment without significantly affecting its mechanical properties and durability. The lightness and the color indexes of treated wood are similar to the ancient wood sample. The mechanical properties of $FeCl_3$ treated wood are not statistically different from the control. Our durability testing results indicated that $FeCl_3$ treated wood has good decay resistance against *Irpex lacteus* and *Trametes versicolor* with a mass loss of less than 10 %. This study provides a convenient method for the restoration and protection of ancient buildings.

Keywords: Ancient wood, fungal resistance, historic timber structures, inorganic salt, mechanical properties.

INTRODUCTION

As history and culture carriers, ancient Chinese architecture is a combination of feng shui, philosophy, art and technology, which is of great significance to cultural inheritance and is worth being protected in many aspects (Yin 2019). These ancient Chinese architecture buildings are mainly in wooden structures, including temples (Li and Zhang 2007), courtyards (Li and Lian 2021), wooden pagodas (Du *et al.* 2002), palaces (Sun

[1]Zhejiang A&F University. College of Chemistry and Materials Engineering. Hangzhou, China.
[2]University of Idaho. Department of Forest, Rangeland and Fire Sciences. Idaho, Moscow. USA.
♠Corresponding author: yuyouming@zafu.edu.cn
Received: 15.12.2021 Accepted: 02.03.2023

2010), etc. However, due to the anisotropic feature of wood, intrinsic susceptibility of wood to deterioration and vandalism of the historical architectures, the present situation of ancient wooden buildings protection is not optimistic (Yang *et al.* 2020, Zhang *et al.* 2013).

The common damage of these historic timber structures includes structural deformation, cracking and decay (Shi and Yong 2014). To solve these problems, there are several established methods to repair or reinforce ancient wooden structures, depending on the degree of damage. The minor damaged part of the wooden building is typically filled with wood flour, unsaturated polyester resins, fiber-reinforced polymers (Zhao *et al.* 2019), carbon nanotubes (Marzi 2015) or other chemical materials (Cao *et al.* 2015) while in more severe cases, the damaged wood structures are usually reinforced with metal-based materials or tensile bars. In terms of completely decayed wooden components, new wood parts or other materials (Chun *et al.* 2013, Que *et al.* 2017) will be used. For example, Yan *et al.* (2012) found that the seismic behavior of the timber-framed structure can be reinforced with iron hooks. Triantafillou and Deskovic (1992) reported that wooden beams that were externally bonded with fiber-reinforced plastic sheets using epoxy adhesives have strengthened performance. Zhou *et al.* (2020)'s research revealed that ethyl orthosilicate and methyl triethoxysilane improved the performance of decayed wood. Although these approaches preserve the structural integrity of the wooden structures, they all greatly affect the aesthetic appearance of ancient buildings. Using wood elements that have a similar color to the ancient wooden building is the most simple and sustainable way to repair and restore damaged wooden structures while allowing for their enhanced cultural and aesthetic values.

Since most methods available for historic timber structures protection significantly affect their original appearance and aesthetic value, and finding wood elements that are similar to the ones in existing historic timber structures is not easy, we propose a method of archaizing wood without damaging the mechanical properties and durability of wood. This idea is based on previous reports by manipulating inorganic salt treatment on wood, the color of treated wood could be as close to the one in the existing wooden building while not significantly affecting the overall performance of wood (Dong 2016, Wang 2017). For example, it was found that the surface color of Chinese fir and larch is closely related to the treating concentration of sodium hydroxide (Dong 2016) and by using different inorganic salts, and treating procedures, the color of wood can reach the target color while not significantly affecting the mechanical properties of wood (Wang 2017). However, the use of multistep inorganic salt treatments, including sodium hydroxide (NaOH), sodium sulfite (Na_2SO_3) and $FeCl_3$, for wood coloration and how these treatments affect the mechanical properties and durability of wood have not been reported (Chen *et al.* 2005).

Castanopsis sclerophylla is very common evergreen broad-leaved tree species in South China which also exhibit good comprehensive performance. (Ding *et al.* 2020) It has been widely used as the material for buildings, bridges and furniture more than 700 years in China. Therefore, in this paper, *Castanopsis sclerophylla* was chosen as the raw material to investigate antique mechanism for the repairment of ancient buildings. The objectives of this study are to investigate the effect of the above-mentioned inorganic salt treatments on the chemical structure of hardwood, *Castanopsis sclerophylla*, which was frequently used as pillars and purlins of beams (Yang 2019) in historic wooden structures. The changes in color, mechanical properties and durability against white-rot wood decay fungi were also reported.

MATERIALS AND METHODS

Materials

Sapwood specimens of *Castanopsis sclerophylla* with no visible defects were cut into various sizes. The size of the samples for flexural test, compressive strength parallel to grain test and soil block test was 10 mm × 10 mm × 150 mm ($R \times T \times L$), 10 mm × 10 mm × 15 mm ($R \times T \times L$) and 14 mm × 14 mm × 14 mm ($R \times T \times L$), respectively. These samples were conditioned at room temperature with a relative humidity of 50 % to constant weight before further analysis.

Sodium hydroxide (NaOH), sodium sulfite (Na_2SO_3), ferric chloride ($FeCl_3$) and hydrochloric acid (HCl) were purchased from Shanghai Aladdin Bio-Chem Technology Co., LTD for inorganic salt treatment. All these chemicals were of chemical grade. Two white-rot fungi, *Irpex lacteus* (*I.l.*) and *Trametes versicolor* (*T.v.*) were obtained from ATCC (Manassas, VA).

$FeCl_3$ treatment on wood

The inorganic salt treatment of wood includes two steps, as shown in Figure 1. Briefly, before $FeCl_3$ solution treatment and to increase the permeability of the wood, the wood samples were soaked in a mixed solution of 2 M NaOH and 0,5 M Na_2SO_3 at 60 ºC for 2 min. Subsequently, the pretreated wood samples were immersed in 0,1 M HCl for 1 min to neutralize the residual alkaline solution on the surface of wood and were further soaked in 0,1 M $FeCl_3$ solution for 5 min to 10 min at room temperature, depending on the sample sizes. The samples were left at room conditions until constant mass.

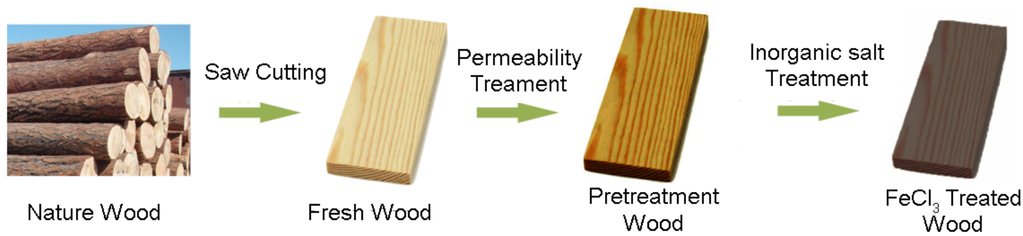

Figure 1: The flow diagram for $FeCl_3$ treatment on wood.

FTIR analysis

Fourier transform infrared spectrometer (NICOLET IMPACT410, NICOLET, Madison, Wisconsin, USA) was used to identify the functional groups of the components. Both the untreated and $FeCl_3$ treated samples were mixed with potassium bromide (KBr) at a weight ratio of 1:100 and pressurized using a tableting method. The IR spectra were recorded with a scanning wavenumber range of 400 cm^{-1} - 4000 cm^{-1} and a scanning resolution of 32. The treated samples were collected from 1 mm below the surfaces of wood along the growth direction and were grounded into 200 mesh before mixing with KBr. The spectra were baseline-corrected and normalized before analysis.

Static bending test and compression parallel to grain

Flexural properties of the $FeCl_3$ treated wood samples were determined through a three-point static bending test using an Instron (Instron 5967, Norwood, MA). A load of 30 kN was applied at a crosshead speed of 5 mm/min to obtain a load-deflection curve. The maximum load at the proportional limit of the curve and the failure curve were used to calculate the modulus of rupture (MOR) and modulus of elasticity (MOE) GB/T 1936.1-2009 (SAC 2009a), GB/T 1936.2-2009 (SAC 2009b), respectively. The corresponding equations were listed below (Equation 1 and Equation 2):

$$\text{Modulus of Rupture}\left(\text{MOR}\right)=\frac{3F_{max}l}{2bt^2} \quad (1)$$

$$\text{Modulus of Elasticity}\left(\text{MOE}\right)=\frac{l^3}{4bt^3}\times\frac{\Delta F}{\Delta f} \quad (2)$$

Where b and t are the width and thickness of the specimen, respectively; l is the span of support, which is 120 mm; F_{max}, ΔF and Δf are load at failure, load increment and deflection increment, respectively.

For compressive strength parallel to the grain test, the wood samples were placed in the center of the spherical moving support of the testing machine and a load of 30 kN at a crosshead rate of 1 mm/min was applied to the samples. The compressive strength of the samples was calculated per the following equation (Equation 3) GB/T 1935-2009 (SAC 2009c):

$$\text{Compressive Strength Paralle to Grain of Wood}\left(\sigma\right)=\frac{P_{max}}{bt} \quad (3)$$

Where σ, P_{max}, b and t are strength parallel to the grain of wood, load at failure, width and thickness of the specimen, respectively.

Color change after inorganic salt treatment

Color evaluation of the wood samples before and after treatment was determined in the CIE $L^*a^*b^*$ color space by a colorimeter (DC-P3) (Janin 1994). L^* means the lightness from black (0) to white (100) while a^* and b^* represent chromaticity indices where $+a^*$ is red, $-a^*$ is green, $+b^*$ is yellow and $-b^*$ is blue. The total color difference (ΔE*) was defined according to the equation given below (Equation 4):

$$\Delta E^* = \sqrt{(\Delta L^*)^2 + (\Delta a^*)^2 + (\Delta b^*)^2} \quad (4)$$

Where ΔL^*, Δa^*, Δb^* are the difference of L^*, $a^*$and b^* before and after treatment, respectively. All the color measurements were taken in the longitudinal directions with 3 replicates (3 measuring points along the diagonal line for each treatment) and the average value was reported.

Leaching test for $FeCl_3$ treated wood

The leaching of wood samples in water was conducted according to the AWPA E11-16 (AWPA 2016a) with a minor modification on the amount of water used. Briefly, 12 replicate samples of untreated and $FeCl_3$ treated wood cubes were fully submerged and weighed down in 78 mL DI water in a beaker to prevent floating. After 1 hour of immersion, the first leachate was collected and replaced with fresh DI water. The beakers were then placed on an orbital shaker and agitated at 100 rad/min for 6 hours, after which the leachate was again collected and replaced with 78 mL fresh DI water. The procedure was repeated for 24 h, 48 h, and thereafter at 48 h intervals, for a total period of 14 days to collect 9 leachates. The leaching test was conducted at room conditions. After the last leachate was collected, the wet mass of the samples and thereafter the final oven-dried mass of the wood cubes were reordered.

Fungal decay resistance test

Fungal resistance of untreated and $FeCl_3$ treated wood samples was conducted according to AWPA E10-16 (AWPA 2016b) with two modifications. First, malt-agar substrate, instead of soil, was used for the durability test. Another modification was that both unleached and leached specimens were sterilized by spraying 70 % ethanol on the surface of the samples in the laminated hood for 2 h. Both untreated (control) and $FeCl_3$ treated specimens with and without leaching were inoculated onto the top of feeder strips that were covered by actively growing fungus, either *I.l.* and *T.v.* The culture bottles were then incubated in an environmental chamber at 75 % humidity and 25 °C in the dark for eight weeks. At the end of the exposure period, the wet mass and the oven-dried mass of the exposed cubes were recorded. The mass loss was calculated according to the following Equation 5.

$$\text{Mass Loss }\% = \frac{\left(m_{unexpo.} - m_{expo.}\right)}{m_{unexpo.}} x\ 100\ \% \quad (5)$$

Where $m_{unxpo.}$ and $m_{expo.}$ are the oven-dried mass of untreated or treated sample before and after exposure to fungi respectively.

Statistical analysis

The mechanical properties data and durability results were statistically analyzed using Statistical Analysis System software (SAS version 9.4, SAS Institute, Cary, NC). The data were compared using a one-way analysis of variance (ANOVA) at the 95 % confidence level (Littell 1998).

RESULTS AND DISCUSSION

FTIR analysis

Figure 2 shows the FTIR spectra of control and $FeCl_3$ treated samples. In control, the peak at 3438 cm^{-1} is attributed to wood-specific O-H stretching vibration. The peak at 2925 cm^{-1} is due to stretching vibrations of methyl, methylene, or methylene (Zhang *et al.* 2019). The absorption band at 1738 cm^{-1} corresponds to the acetyl group in hemicellulose. The absorption band at 1631 cm^{-1} is related to the stretching vibration of C=O. The peaks at 1511 cm^{-1} and 1464 cm^{-1} correspond to the stretching vibration of the benzene ring caused by the vibration of the lignin aromatic skeleton. Absorption peaks at 1425 cm^{-1} and 1384 cm^{-1} correspond to the C-H deformation in lignin and carbohydrates. After inorganic salt treatment, the peak at 1738 cm^{-1} in the spectrum of the treated sample disappeared, indicating the loss of hemicellulose due to the treatment effect. Moreover, the intensities of the peaks from 1400 cm^{-1} to 1600 cm^{-1} were weakened, possibly related to the partial removal of lignin in $FeCl_3$ treated wood (Zhang *et al.* 2019).

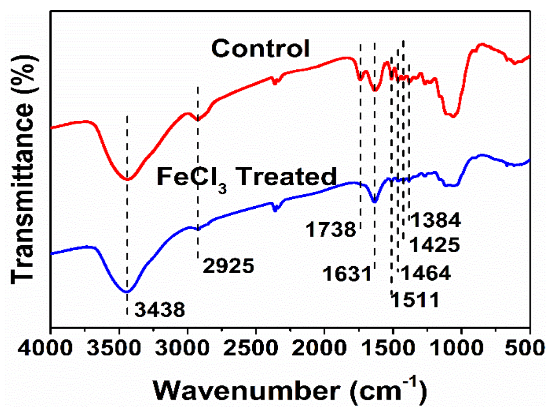

Figure 2: Fourier-transform infrared spectra (FTIR) of untreated and $FeCl_3$ treated samples.

Color measurement

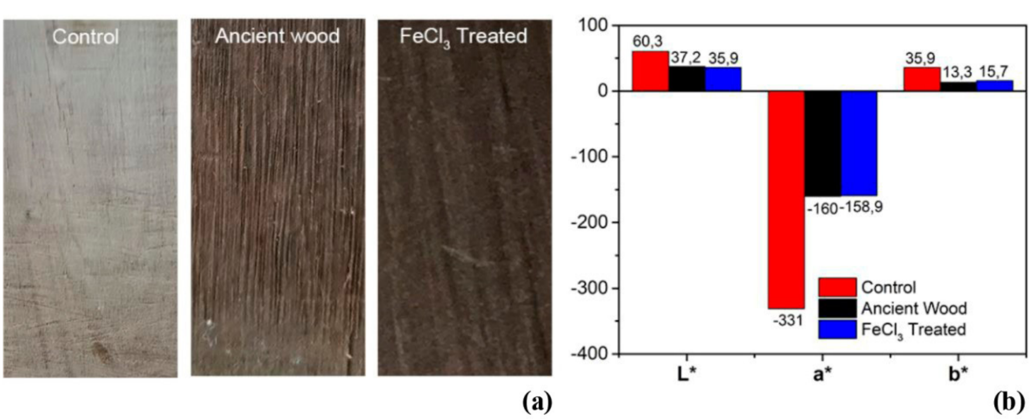

Figure 3: (a) Photos of wood samples before and after treatment, (b) Surface color parameters of control, ancient wood and $FeCl_3$ treated wood samples.

Table 1: The color difference (**ΔE***) of control, ancient wood and $FeCl_3$ treated wood samples.

ΔE*	Control Sample	Ancient wood Sample	Treated Sample
Control Sample	0	172,8	173,9
Ancient Wood Sample	172,8	0	2,9
Treated Sample	173,9	2,9	0

Figure 3a shows images of control, ancient wood and $FeCl_3$ treated wood, with the latter two exhibiting similar color while contrasting to the control. These color differences were further quantified by the colorimeter, as shown in Figure 3b. As compared to the control, the lightness L^* of $FeCl_3$ treated samples is much lower but close to that of ancient wood samples. Similarly, the chromaticity indices a* and b* of the treated sample is comparable with ancient wood samples but redder and bluer than that of the untreated samples. These results indicate that the color of our $FeCl_3$ treated wood resembles that of ancient wood sample, which could be further evidenced by their color difference (**ΔE***), as shown in Table 1.

Mechanical properties of $FeCl_3$ treated wood

The flexural and compression properties of untreated and $FeCl_3$ treated wood are shown in Figure 4. Statistically, the inorganic salt treatment does not significantly affect the MOE, MOR and compression strength of the samples. This is because our pretreatment time is short (Xu *et al.* 2020) and NaOH solution at a lower concentration. Similar results have been reported by Ishikura *et al.* (2010) that the bending properties of the treated Yezo spruce samples were not affected by NaOH solution at a concentration less than 10 %.

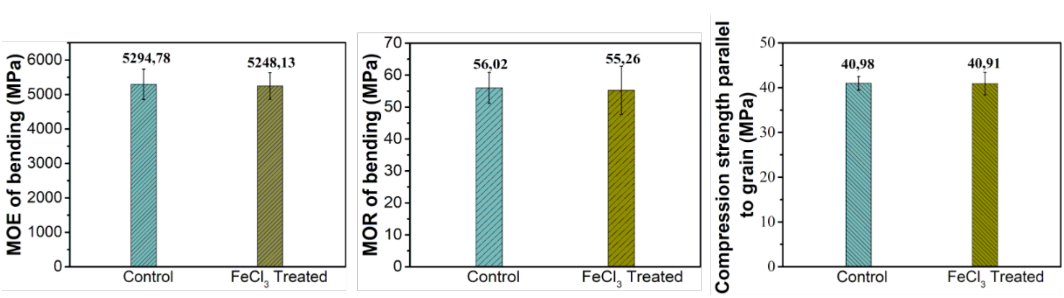

Figure 4: MOE, MOR and compression strength parallel to grain of untreated and $FeCl_3$ treated wood.

Fungal resistance of $FeCl_3$ treated wood against white-rot fungi

Figure 5 shows the mass loss of control and $FeCl_3$ treated wood with and without leaching after 8 weeks of exposure to two common white-rot fungi, *I.l.* and *T.v.*. In the control group, the mass loss of wood samples due to white rot decay without leaching is around 4 % - 7 %, which is significantly higher ($p<0,05$) than those of the samples with leaching (1 % - 4 %). The relatively high mass loss of control samples without leaching could be related to the leaching of extractives from the wood cubes during the fungi exposure period, as evident by the deposition of leachate on the surface of the fungi mycelium in the culture bottles (Figure 5). Similar results were observed for $FeCl_3$ treated samples when exposed to *I.l.,* with leached samples recording the lowest mass loss. In comparison, there is no significant difference in mass loss of treated samples without leaching and with leaching when exposed to *T.v.* ($p>0,05$), although both mass losses are the highest among all the tested samples ($p>0,05$). These results indicate that iron in $FeCl_3$ treated wood might have stimulated the degradation of wood by *T.v.* (Schilling 2010), thus leading to the highest mass loss. The difference in mass loss of treated samples exposed to the two fungi species indicates that the fungal resistance properties of $FeCl_3$ may be fungal specific and hence varies from one fungal to the other. Overall, based on the mass loss results, *Castanopsis sclerophylla* wood samples are resistant to the decay of both *I.l.* and *T.v.* and $FeCl_3$ treatment on this wood does not significantly affect its durability against *I.l.*.

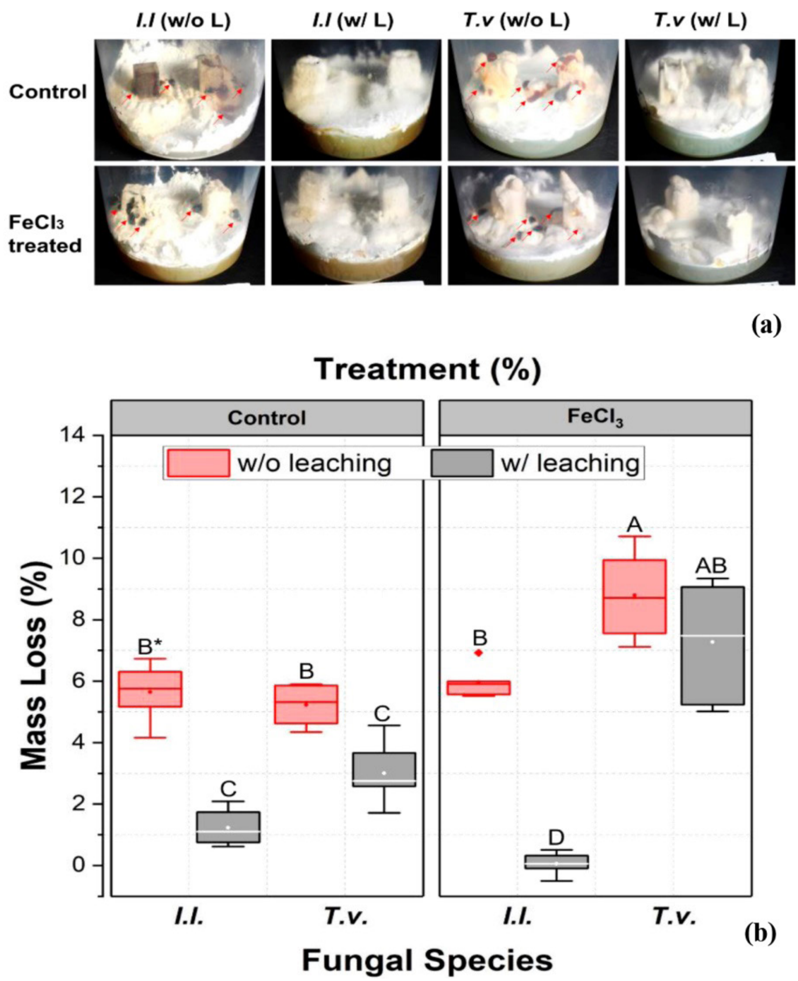

Figure 5: (a) Representative culture bottles, (b) mass loss of control and $FeCl_3$ treated wood with and without leaching after 8-week exposure to *Irpex lacteus (I.l.)* and *Trametes versicolor (T.v.)* in an AWPA E10-16 soil block test. An arrow (↑) was used to indicate the leachates while asterisk (*) means that mass loss with no common letters are significantly different ($p<0,05$).

CONCLUSIONS

This study proposed an effective and facile approach of archaizing wood through inorganic salts treatment. The color of $FeCl_3$ treated wood is very close to the ancient wood sample. The mechanical properties of the treated wood, including MOE, MOR and compression strength parallel to grain, are not significantly different from those in control. The $FeCl_3$ treated wood is also resistant to the decay of *I.l.* and *T.v.* and the mass losses were below 10 %, regardless of the leaching test. Therefore, this is a promising method that could be used for future historic timber buildings repair and protection.

AUTHORSHIP CONTRIBUTIONS

M.S.: Writing, original draft, Visualization Data curation; C.Z.: Visualization, Data curation; C. A.: Visualization, Data curation; Y. Y.: Supervision, Resources; L.C.: Supervision, Writing –review & editing.

ACKNOWLEDGMENTS

The authors are grateful for the financial supports from National Natural Science Foundation of China (No. 32071684), Zhejiang Natural Science Foundation of China (No. LY16C160010), Zhejiang University Student Science and Technology Innovation Activity Plan (New Seedling talent plan subsidy project, No. 2022R412B043) and USDA McIntire-Stennis project under accession number NI3551. Any opinions, findings, conclusions, or recommendations expressed in the publication are those of the authors and do not necessarily reflect the view of the U.S. Department of Agriculture.

REFERENCES

AWPA Technical Committee. AWPA. 2016a. Standard Method for Accelerated Evaluation of Preservative Leaching. AWPA E11-16. AWPA Technical Committee, USA.

AWPA Technical Committee. AWPA. 2016b. Laboratory method for evaluating the decay resistance of wood-based materials against pure basidiomycete cultures: soil/block test. AWPA E10-16. AWPA Technical Committee, USA.

Cao, J.; Wang, J.L.; Li, Y.H.; Wang, S.; Du, D.S.; Dong, M. 2015. In-situ consolidation and restoration of wooden components in historic buildings. *Journal of Northwest University* 30(4): 257- 262. ISSN 1001-7461.

Chun, Q.; Yu, M.Z.; Pan, J.W. 2013. Research on damage characteristic and structural performance of the main hall of Baoguo temple in Ningbo. *Science, conservation and archaeology* 25(2): 45-51. ISSN 1005-1538. https://doi.org/10.16334/j.cnki.cn31-1652/k.2013.02.004

Chen, Y.S.; Liu, X.Y.; Li, H.; Huang, R.F. 2005. Issues concerning the preserving ancient timber structures. *Palace Museum Journal* (5): 332-343. ISSN 0452-7402.

Du, J.K.; Feng, X.Z.; Wang, Z.L.; Huang, Y.S.; Ramadan, E. 2002. The methods of extracting water information from spot image. *Chinese Geographical Science* 12(1): 68-72. https://doi.org/10.1007/s11769-002-0073-1

Dong, Z.Q. 2016. Study on the mechanism of inorganic salt accelerated aging wood. M.S. Thesis, Zhejiang A&F university, Hangzhou, China.

Ding, Y.; Wan, J.; Liu, C.; Shi, X.; Xia, X.; Prakash, S.; Zhang, X. 2020. Retrogradation properties and in vitro digestibility of wild starch from *Castanopsis sclerophylla*. *Food Hydrocolloids* 103: e105693. https://doi.org/10.1016/j.foodhyd.2020.105693

Ishikura, Y.; Abe, K.; Yano, H. 2010. Bending properties and cell wall structure of alkali-treated wood. *Cellulose* 17(1): 47-55. https://doi.org/10.1007/s10570-009-9360-7

Janin, G. 1994. *Colorimétrie: principe de la mesure de la couleur*. Application au bois. Le bois: matériau d'ingénierie. ARBOLOR: Lorraine, France 10: 379-399. https://hal.inrae.fr/hal-02843775

Li, J.; Zhang, F. 2007. The characteristic research of the Hunan temple construction. *Chinese and Overseas Architecture* 4: 71-73. ISSN 1008-0422. http://caod.oriprobe.com/articles/12369013/The_characteristic_research_of_the_Hunan_temple_construction.htm

Li, Y.J.; Lian, M.C. 2021. Analysis on the layout of traditional residential courtyards and building structures in Guanzhong area, Shaanxi-Taking Xiaojiapo village in Lantian county as an example. In *IOP Conference Series: Earth and Environmental Science* 768(1): e012141. https://doi.org/10.1088/1755-1315/768/1/012141

Littell, R.C.; Henry, P.R.; Ammerman, C.B. 1998. Statistical analysis of repeated measures data using SAS procedures. *Journal of Animal Science* 76(4): 1216-1231. https://doi.org/10.2527/1998.7641216x

Marzi, T. 2015. Nanostructured materials for protection and reinforcement of timber structures: A review and future challenges. *Construction and Building Materials* 97: 119-130. https://doi.org/10.1016/j.conbuildmat.2015.07.016

Que, Z.; Li, Z.; Zhang, X.; Yuan, Z.; Pan, B. 2017. Traditional wooden buildings in China. Chapter 10. In *Wood in Civil Engineering*. Concu, G. (Ed.). 250p. IntechOpen Limited, London: UK. https://doi.org/10.5772/66145

Sun, Y. 2010. Intercommunity of architectural design concepts of Chinese ancient palaces from the perspective of the Imperial Palace. *Shanxi Archi* 36(29): 18-19. ISSN 1009-6825

Shi, H.; Yong, Z.H. 2014. Study on ancient architecture reparation technology. *Suzhou University of Science and Technology* 27(4): 68-72. ISSN 2096-3270.

SAC. 2009a. Method of testing in bending strength of wood. GB/T 1936.1-2009. Research Institute of Wood Industry, Chinese Academy of Forestry: China.

SAC. 2009b. Method for determination of the modulus of elasticity in static bending of wood. GB/T 1936.2-2009. Research Institute of Wood Industry, Chinese Academy of Forestry: China.

SAC. 2009c. Method of testing in compressive strength parallel to grain of wood. GB/T 1935-2009. Research Institute of Wood Industry, Chinese Academy of Forestry: China.

Schilling, J.S. 2010. Effects of calcium-based materials and iron impurities on wood degradation by the brown rot fungus Serpula lacrymans. *Holzforschung* 64(1): 93-99. https://doi.org/10.1515/hf.2010.009

Triantafillou, T.C.; Deskovic, N. 1992. Prestressed FRP sheets as external reinforcement of wood members. *Journal of Structural Engineering* 118(5): 1270-1284. https://doi.org/10.1061/(asce)0733-9445(1992)118:5(1270)

Wang, C. 2017. Study on the mechanism of multi-inorganic salt accelerated aging wood. M.S. Thesis, Zhejiang A&F university, Hangzhou, China.

Xu, E.; Wang, D.; Lin, L. 2020. Chemical structure and mechanical properties of wood cell walls treated with acid and alkali solution. *Forests* 11(1): e87. https://doi.org/10.3390/f11010087

Yin, Y.R. 2019. The integration mechanism of ancient architecture protection and modern construction. *E3S Web of Conferences* 136: e04036. https://doi.org/10.1051/e3sconf/201913604036

Yang, R.Y.; Sun, Y.F.; Zhang, X.F. 2020. Application and progress of reinforcement technology for Chinese ancient buildings with wood structure. *Geotechnical and Geological Engineering* 38: 5695-5701. https://doi.org/10.1007/s10706-020-01433-z

Yan, W.M.; Zhou, Q.; Zhang, B.; Li, Z.B. 2012. Aseismic behavior of chinese ancient wooden structure strengthened by iron-hook. *Journal of Beijing University of Technology* ISSN:0254-0037. 38(4): 502-508.

Yang, J. 2019. From materials: enlightenment of wood selection and application in ancient Chinese timber buildings. *The Architect* 4: 101-106. ISSN1001-6740.

Zhang, H.M.; Yang, S.G.; Zhang, Y.J.; Lu, X.; Li, Y.F.; Tao, B. 2013. Characteristics of ancient building lightning disasters. *Meteorological Sci Technology* 41(4): 758-763. ISSN:1671-6345. https://doi.org/10.19517/j.1671-6345.2013.04.027

Zhao, X.B.; Zhang, F.L.; Xue, J.Y.; Ma, L.L. 2019. Shaking table tests on seismic behavior of ancient timber structure reinforced with CFRP sheet. *Engineering Structures* 197: e109405. https://doi.org/10.1016/j.engstruct.2019.109405

Zhou, K.; Li, A.; Xie, L.L.; Wang, C.C.; Wang, P.; Wang, X.F. 2020. Mechanism and effect of alkoxysilanes on the restoration of decayed wood used in historic buildings. *Journal of Cultural Heritage* 43: 64-72. https://doi.org/10.1016/j.culher.2019.11.012

Zhang, T.; Yang, P.; Chen, M.Z.; Yang, K.; Cao, Y.Z.; Li, X.H.; Tang, M.; Chen, W.M.; Zhou, X.Y. 2019. Constructing a novel electroluminescent device with high-temperature and high-humidity resistance based on a flexible transparent wood film. *ACS Applied Materials & Interfaces* 11(39): 36010-36019. https://doi.org/10.1021/acsami.9b09331.